Cancer-associated fibroblasts enact field cancerization by promoting extratumoral oxidative stress

Jeremy Soon Kiat Chan*[,1], Ming Jie Tan[1,6], Ming Keat Sng[1], Ziqiang Teo[1], Terri Phua[1,2], Chee Chong Choo[1], Liang LI[1], Pengcheng Zhu*[,1] and Nguan Soon Tan*[,1,3,4,5]

Histological inspection of visually normal tissue adjacent to neoplastic lesions often reveals multiple foci of cellular abnormalities. This suggests the presence of a regional carcinogenic signal that spreads oncogenic transformation and field cancerization. We observed an abundance of mutagenic reactive oxygen species in the stroma of cryosectioned patient tumor biopsies, indicative of extratumoral oxidative stress. Diffusible hydrogen peroxide (H_2O_2) was elevated in the conditioned medium of cultured skin epithelia at various stages of oncogenic transformation, and H_2O_2 production increased with greater tumor-forming and metastatic capacity of the studied cell lines. Explanted cancer-associated fibroblasts (CAFs) also had higher levels of H_2O_2 secretion compared with normal fibroblasts (FIBs). These results suggest that extracellular H_2O_2 acts as a field effect carcinogen. Indeed, H_2O_2-treated keratinocytes displayed decreased phosphatase and tensin homolog (PTEN) and increased Src activities because of oxidative modification. Furthermore, treating FIBs with CAF-conditioned medium or exogenous H_2O_2 resulted in the acquisition of an oxidative, CAF-like state. *In vivo*, the proliferative potential and invasiveness of composite tumor xenografts comprising cancerous or non-tumor-forming epithelia with CAFs and FIBs could be attenuated by the presence of catalase. Importantly, we showed that oxidatively transformed FIBs isolated from composite tumor xenografts retained their ability to promote tumor growth and aggressiveness when adoptively transferred into new xenografts. Higher H_2O_2 production by CAFs was contingent on impaired TGFβ signaling leading to the suppression of the antioxidant enzyme glutathione peroxidase 1 (GPX1). Finally, we detected a reduction in Smad3, TAK1 and TGFβRII expression in a cohort of 197 clinical squamous cell carcinoma (SCC) CAFs, suggesting that impaired stromal TGFβ signaling may be a clinical feature of SCC. Our study indicated that CAFs and cancer cells engage redox signaling circuitries and mitogenic signaling to reinforce their reciprocal relationship, suggesting that future anticancer approaches should simultaneously target ligand receptor and redox-mediated pathways.

Tumor initiation, growth and propagation are frequently accompanied by desmoplasia and the acquisition of a reactive stroma mainly comprising cancer-associated fibroblasts (CAFs).[1–3] The dynamic and reciprocal relationship between the epithelial and mesenchymal compartments of the tumor dictates almost every aspect of cancer progression, even governing the efficacy of therapy and influencing the risk of disease relapse.[4,5] Importantly, a population of epithelial and stromal cells adjacent to the primary neoplastic lesion acquires early genetic changes but lacks histopathology, indicating that tumors prime the surrounding tissue for malignancy, an effect known as field cancerization.[6,7] Field cancerization results in multifocal primary tumors in close proximity with a higher chance of recurrence after surgical resection of malignant tumors.[8] Although genetic and epigenetic anomalies have been well described as the driving force behind field cancerization of premalignant epithelia,[6] mediators of field cancerization by the stroma remain poorly understood.

The expansion of the cancer field requires soluble factors that promote oncogenic transformation in a non-cell-autonomous manner and prime the adjacent naïve stroma to support tumor growth. Although these functions are usually ascribed to growth factors and cytokines, reactive oxygen species (ROS), which are persistently elevated in almost all cancers, have been recently identified as critical intermediates of cellular signaling.[9–11] The oxidative modification of proteins by ROS modulates intracellular signaling to influence cellular behavior and contribute to the pathophysiology of many human diseases.[12,13] ROS are by-products of aberrant metabolism in the tumor epithelia, and their cell-autonomous mutagenic effects have been studied extensively. Much less is known about the regulation of ROS in CAFs and how ROS impact field cancerization. Notably, not all ROS are well suited for paracrine cell signaling. Superoxide anions (O_2-) and hydroxyl radicals (OH•) have a very short diffusion distance because they are highly reactive, resulting in a very short half-life in the aqueous phase.[14] They also have a very low permeability coefficient for lipid bilayers.[15] In contrast,

[1]School of Biological Sciences, Nanyang Technological University, 60 Nanyang Drive, Singapore; [2]Department of Microbiology, Tumor and Cell Biology, Karolinska Institutet, Nobelsväg 16, Stockholm, Sweden; [3]Lee Kong Chian School of Medicine, Nanyang Technological University, 50 Nanyang Avenue, Singapore; [4]Institute of Molecular and Cell Biology, A*STAR, 61 Biopolis Drive, Proteos, Singapore and [5]KK Women's and Children Hospital, 100 Bukit Timah Road, Singapore
*Corresponding author: JSK Chan or P Zhu or NS Tan, School of Biological Sciences, Nanyang Technological University, 60 Nanyang Drive, Singapore 637551, Singapore;
Tel: +65 63162941; Fax: +65 67913856; E-mail: CHAN0693@e.ntu.edu.sg or PCZhu@ntu.edu.sg or nstan@ntu.edu.sg
[6]Current address: DeNova Sciences Pte Ltd, 16 Nanyang Drive, Innovation Centre Blk 1, Singapore 637722, Singapore.
Received 14.9.16; revised 22.12.16; accepted 22.12.16; Edited by A Finazzi-Agro'

hydrogen peroxide (H_2O_2) has a longer half-life, is lipid soluble and can diffuse across the cellular plasma membrane, making it an ideal field effect carcinogen. In this study, we investigated the regulation of ROS, and in particular, H_2O_2 production, in CAFs and how this tumor stroma-mediated oxidative stress causes a premalignant field defect.

Results

Elevated ROS in the microenvironment of numerous tumor types. We first examined the oxidative status of tumor sections from patients with late stage (stage 3 to metastatic) skin squamous cell carcinoma (SCC), gastric, breast and colon cancers using the ROS-sensitive fluorescent dye CM-H_2DCFDA. Pan-cytokeratin staining distinguished between tumor epithelia and stromal elements. All tumor sections stained positive for ROS (Figure 1a). SCC sections exhibited the highest intensity of ROS staining. Interestingly, ROS were not restricted to the tumor epithelia but were frequently observed in the stromal compartments of tumors. To identify the cell types responsible for elevated microenvironmental ROS, we measured extracellular H_2O_2 in conditioned medium from various SCC lines of different aggressiveness

(Figure 1b). HaCaT is a non-tumorigenic human keratinocyte cell line, whereas benign A-5, malignant II-4 and highly aggressive A-5RT3 are sublines of different tumorigenic potential derived from HaCaT cells.[16] HaCaT cells secreted the lowest amount of H_2O_2, whereas conditioned medium from A-5RT3 cells had the highest level of H_2O_2 (Figure 1b). As CAFs dominate the tumor stroma and diffusible H_2O_2 is well suited for a role in tumor stroma crosstalk, we measured the amount of H_2O_2 in conditioned medium from CAFs explanted from four patient skin SCC biopsies alongside their paired normal fibroblasts (FIBs) (Figure 1c). We consistently detected higher extracellular H_2O_2 in the conditioned medium from SCC CAFs compared with FIBs.

Microenvironment oxidative stress causes a premalignant field defect. Next, we determined whether microenvironmental oxidative stress promotes premalignant development, that is, field cancerization. As the tumor promotion protocol involves a mutagen, *N*-methyl-*N'*-nitro-*N*-nitrosoguanidine (MNNG), we first determined the cytotoxic dose of MNNG in combination with various concentrations of H_2O_2. There were no significant differences in the percentages of apoptotic (Annexin V^{high}/PI^{low} and Annexin V^{high}/PI^{high}) and
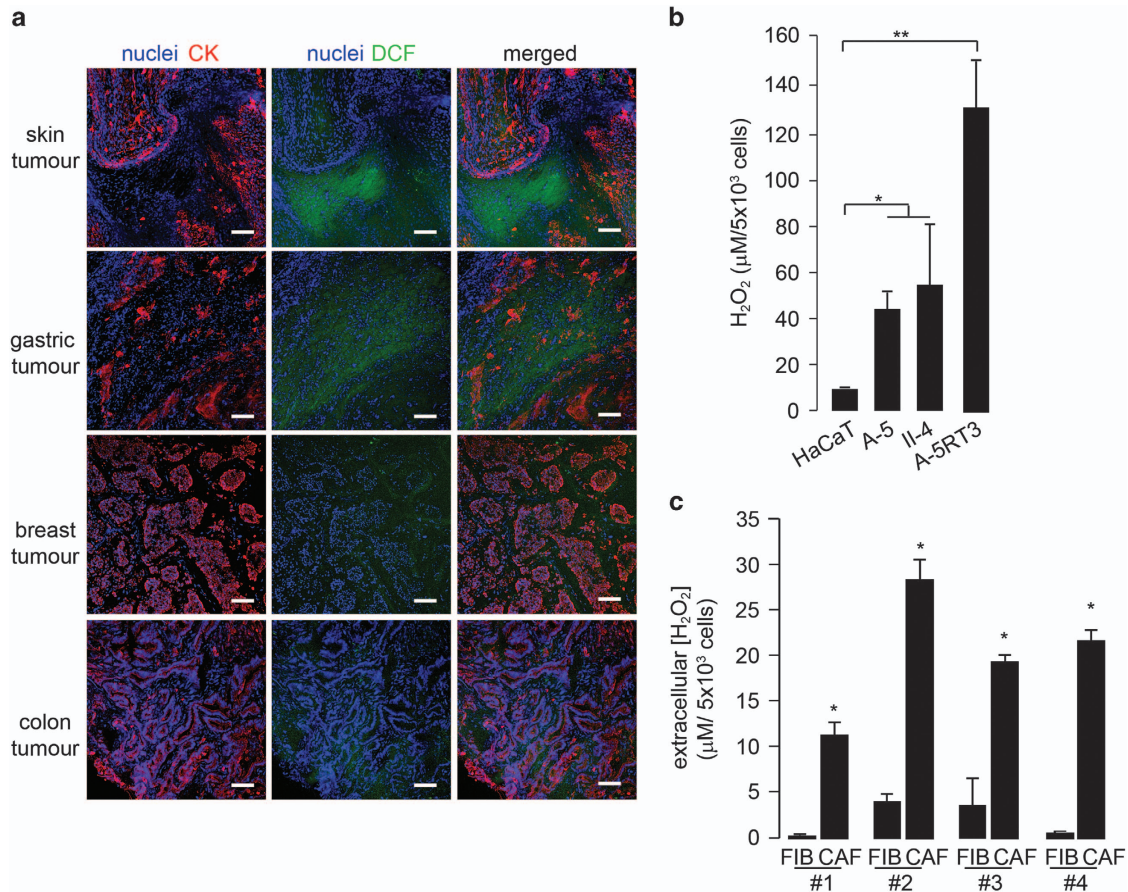

Figure 1 Elevated ROS in the microenvironment of numerous tumor types. (**a**) Dichlorofluorescein diacetate (DCF) staining to detect ROS on sections of patient tumor biopsies from the skin, gastric, breast and colon. Pan-cytokeratin (CK) antibody staining was used to delineate epithelial-stromal boundaries. Sections were counterstained with DAPI. Scale bar: 100 μm. (**b** and **c**) Extracellular concentrations of H_2O_2 in the conditioned medium from **b**, various human SCC lines, and (**c**) paired FIBs and CAFs from human SCC explants, as measured by Amplex Red H_2O_2 assay. *$P < 0.05$, **$P < 0.01$
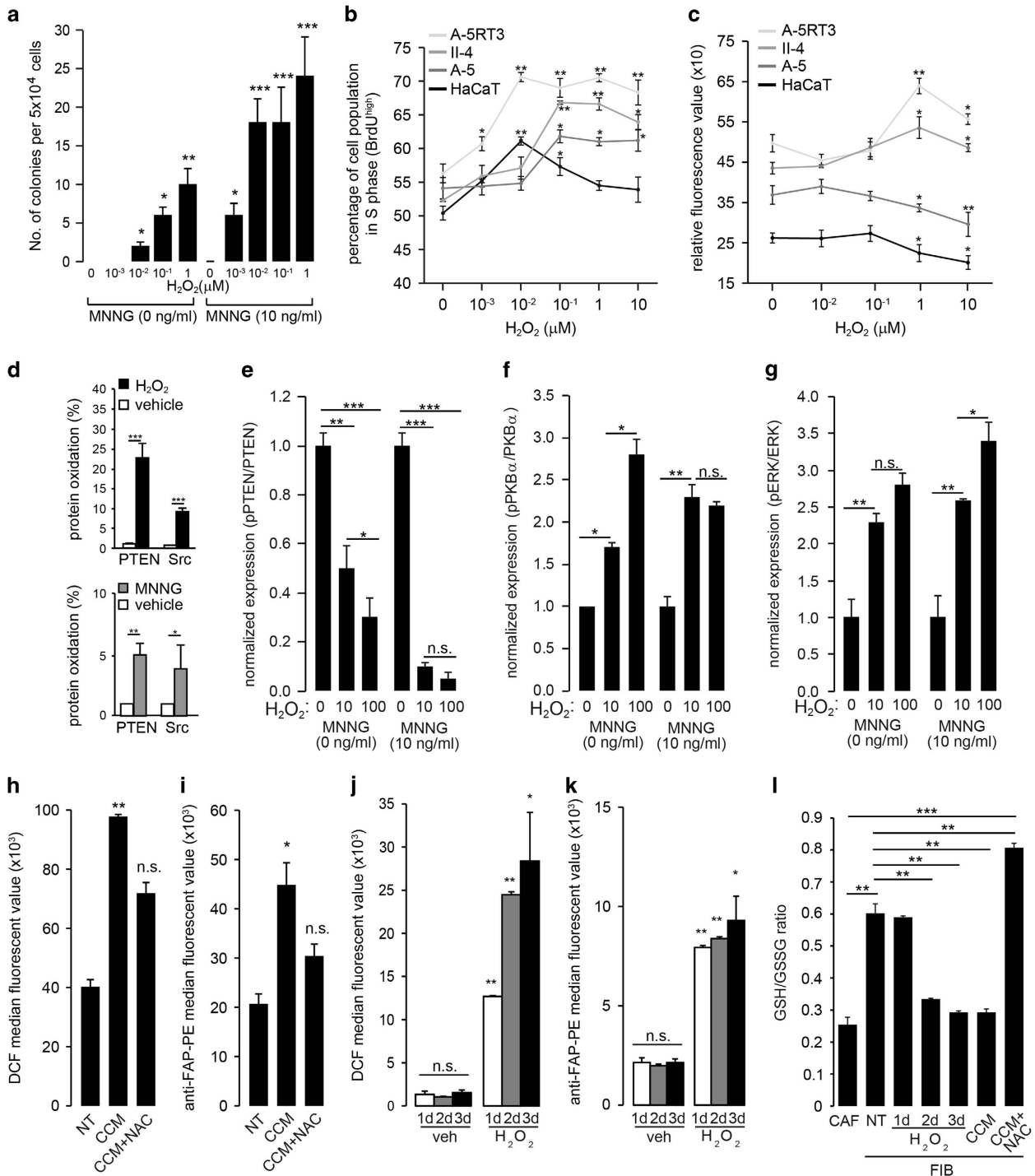
Figure 2 H_2O_2 has a transforming effect on epithelia and fibroblasts *in vitro*. (**a**) Quantification of epithelial colonies in soft agar at 1 month after the indicated treatments with MNNG and H_2O_2. (**b**) Percentages of proliferating (S-phase) cells after the indicated treatments with H_2O_2 as determined by BrdU labeling and FACS analysis. (**c**) Relative fluorescence (SYTO60 dye) readings of invaded cells after the indicated treatments in the transwell invasion assay. (**d**) PEG-switch assay followed by immunoblot analysis of oxidatively modified PTEN and Src in keratinocyte lysates subjected to the indicated treatments. Bars represent the percentage of protein targets that have undergone oxidative modification. (**e**-**g**) Immunoblot analysis of key signaling mediators of the PI3K and ERK pathways in keratinocytes subjected to the indicated treatments. Bars represent normalized densitometry measurements of phosphorylated protein targets normalized against the cognate unphosphorylated forms. (**h**–**k**) Median fluorescence intensities of human fibroblasts subjected to the indicated treatments, followed by staining with DCF and PE-conjugated anti-FAP antibody and FACS analysis. (**l**) Measurements of GSH/GSSG ratio in CAF and FIBs subjected to the indicated treatments. A low GSH/GSSG ratio is an indicator of oxidative stress in cells. The data are presented as the mean ± S.D. of three independent experiments. Statistical tests were performed against cognate untreated cells for each cell type. NS, not significant, *$P < 0.05$, **$P < 0.01$, ***$P < 0.001$

necrotic (AnnexinV^{low}/PI^{high}) keratinocytes treated with 1–100 nM H_2O_2 alone or in combination with 10 ng/ml MNNG (Supplementary Tables S2 and S3). Thus, this range of H_2O_2 and MNNG was used to examine the effects of H_2O_2 on

colony formation in soft agar. A marked increase in colony number was observed with cells pretreated with MNNG and exposed to H_2O_2 for 4 weeks (Figure 2a). Keratinocytes treated with a higher concentration of H_2O_2 alone formed
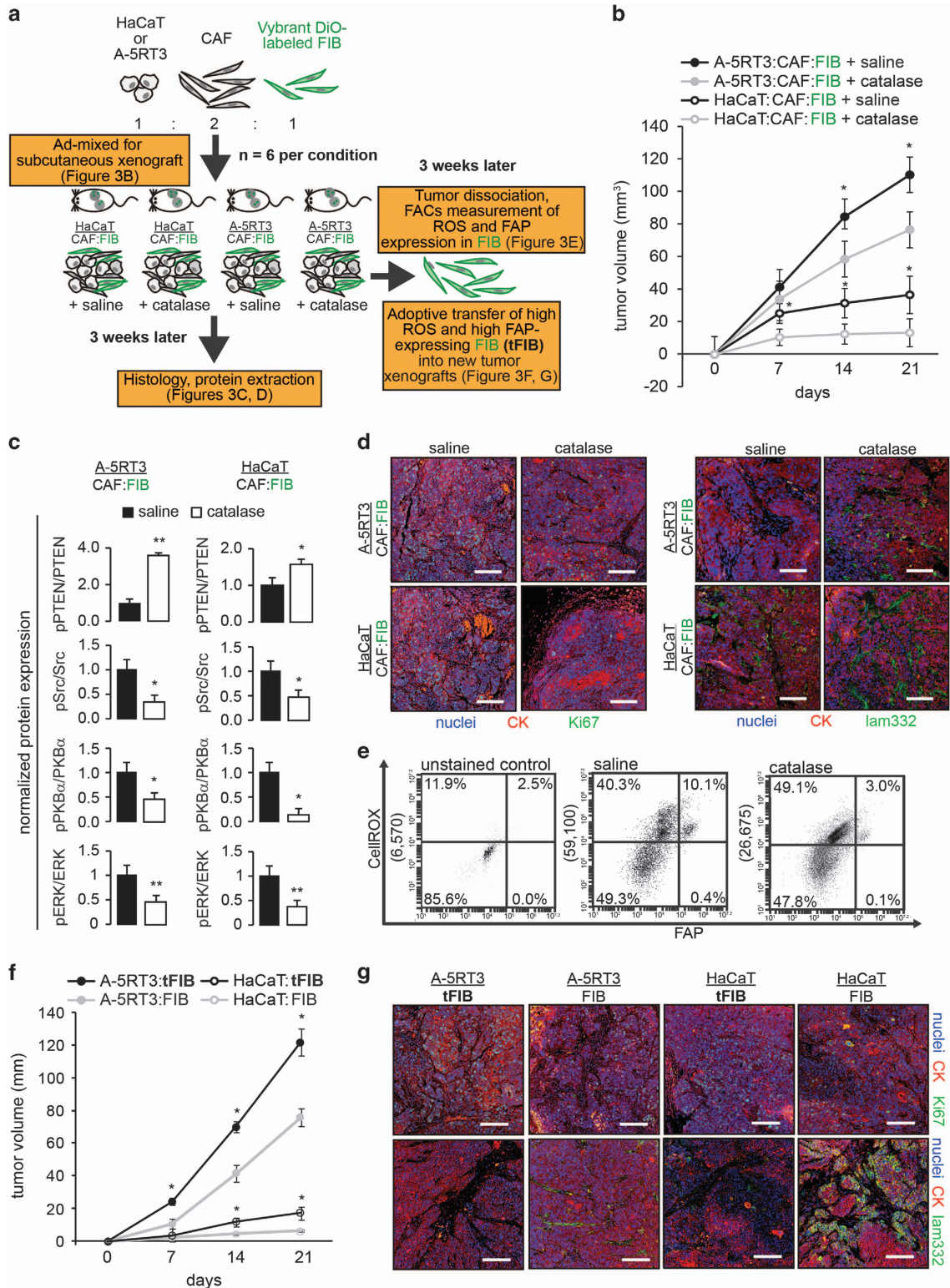
colonies in soft agar, suggesting that chronic exposure to elevated extracellular H_2O_2 facilitates the transformation of epithelial cells. It is conceivable that normal and neoplastic epithelial cells respond differently to H_2O_2. Indeed, we observed differential growth response and invasiveness to exogenous H_2O_2. The proliferation of HaCaT and A-5RT3 cells peaked at 10 nM H_2O_2, whereas the proliferation of A-5 and II-4 cells peaked at 100 nM H_2O_2. The proliferation of HaCaT cells began to decrease as the concentration of H_2O_2 increased to 10 μM. In contrast, the growth of the three tumorigenic sublines remained significantly elevated compared with untreated cognate controls (Figure 2b). Exogenous H_2O_2 also increased the invasiveness of the malignant II-4 and A-5RT3 cells, whereas that of normal HaCaT and benign A-5 cells was reduced as determined by a transwell invasion assay (Figure 2c). The differential growth response and invasiveness was not due to H_2O_2-induced apoptosis, as apoptosis of the cell lines was only observed at H_2O_2 concentrations >100-fold higher than those used for the proliferation and invasion assays as determined by Annexin V/PI FACS analysis. (Supplementary Figure S1A). These observations indicate that sub-cytotoxic levels of H_2O_2 differentially modulate the behavior of normal and neoplastic epithelial cells.

Next, we performed a polyethylene glycol (PEG)-switch assay on H_2O_2- and MNNG-treated keratinocytes to identify oxidatively modified proteins. As an oxidant, H_2O_2 oxidizes cysteine residues in proteins and modifies their activities. The PEG-switch assay results in the conjugation of PEG to the oxidized cysteine residue, thereby increasing the molecular weight of the oxidized protein and slowing its migration within an SDS-PAGE gel. Proteins bordering the cell membrane are particularly susceptible to modification by extracellular H_2O_2. Phosphatase and tensin homolog (PTEN) and Src are well-established mediators of tumorigenesis that are membrane associated. The oxidation of PTEN forms a disulfide bridge that inactivates its tumor-suppressive catalytic activity;[17,18] Src oxidation increases its autophosphorylation and concomitant activation.[19,20] Indeed, an elevated level of oxidized PTEN and Src in keratinocytes treated with H_2O_2 and MNNG was detected by PEG-switch assay, further confirmed by Oxyblot (Figure 2d, Supplementary Figures S1B and C). MNNG alone only contributed to $\leq 4\%$ of oxidized PTEN and Src, whereas H_2O_2 contributed to $\sim 20\%$ oxidized PTEN and $\sim 10\%$ oxidized Src (Figure 2d). Notably, oxidized JNK and EGFR were also detected by PEG-switch, reflecting the promiscuous nature of H_2O_2 interactions (Supplementary Figure S1D). PTEN and Src participate in the activation of the

PI3K/PKBα and MAPK/ERK signaling pathways, which have pivotal roles in tumor development and progression. Immunoblot analysis confirmed increased activation of downstream mediators of the PI3K/PKBα and MAPK/ERK pathways (Figures 2e-g, Supplementary Figure S1E). A focused qPCR array comparing H_2O_2-treated epithelia and those cocultured with CAFs revealed similar altered expression profiles of many pro-oncogenic and pro-tumor genes. Similarly, the expression of tumor suppressors and growth inhibitory mediators was reduced (Supplementary Figure S1F).

In addition to epithelial cells, H_2O_2 may promote field cancerization by affecting adjacent FIBs. We first investigated whether CAF-conditioned medium (CCM) alters the behavior of FIBs. FIBs cultured in CCM had increased ROS levels and elevated expression of fibroblast-activated protein (FAP), a biomarker of CAFs (Figures 2h-i, Supplementary Figures S2A and B). This effect can be attributed, partially, to extracellular ROS because H_2O_2 was detected in CCM (Supplementary Figure S2C), and the increase in CAF marker expression was attenuated when CCM was pretreated with the antioxidant NAC. Similar experiments were also performed using H_2O_2 alone. Normal FIBs exposed to exogenous H_2O_2 also displayed elevated ROS and increased FAP levels after 1 day, and αSMA expression was increased after 3 days (Figures 2j-k, Supplementary Figure S2D-F). Consistently, analysis of the GSH:GSSG ratio revealed that CAFs and H_2O_2- or CCM-treated FIBs experienced oxidative stress (reflected by a low GSH:GSSG ratio) compared with non-treated FIBs. NAC increased the GSH:GSSG ratio of CCM-treated FIBs (Figure 2l). These collective observations suggest that extratumoral H_2O_2 is a transformative agent in stromal field cancerization, stimulating genetic and phenotypic changes in the epithelial cells and normal stromal fibroblasts to generate a field effect.

Oxidative transformation of FIBs to CAF-like cells was attenuated by catalase *in vivo*. To determine whether extratumoral H_2O_2 generates a field effect *in vivo*, we generated an admixed tumor xenograft containing three different cell types, namely, epithelial cells, CAFs and VybrantDiO-labeled FIBs, in the presence or absence of 500 U/ml extracellular catalase (Figure 3a). Cancerous A-5RT3 cells with CAFs:FIBs formed large tumors, whereas non-tumorigenic HaCaT cells with CAFs:FIBs formed small palpable neoplasms (Figure 3b). Notably, tumor growth was attenuated by catalase in the microenvironment (Figure 3b). Consistent with the *in vitro* observations, the tumor xenografts showed reduced activation of key mediators of the

Figure 3 H_2O_2 promotes field cancerization *in vivo*. (**a**) Schematic of the experimental approach using VybrantDiO-labeled fibroblasts (FIBs) and CAFs for subcutaneous tumor xenografts in NSG mice. (**b**) Volume measurements of tumor xenografts injected with or without catalase. Statistical tests were performed against cognate saline-treated xenografts. (**c**) Immunoblot analysis of phospho-PTEN, phospho-Src and downstream signaling mediators from tumor lysates. Bars represent normalized densitometry measurements of phosphorylated protein targets normalized against the cognate unphosphorylated forms. (**d** and **g**) Immunofluorescence staining for the proliferation marker Ki67 and the basal lamina protein laminin 332. Pan-cytokeratin (CK) antibody staining was used to delineate epithelial-stromal boundaries. Sections were counterstained with DAPI. Scale bar = 100 μm. (**e**) Representative scatterplot for tumor cells stained with CellROX and PE-conjugated FAP antibody. Only VybrantDiO-labeled FIBs were gated for analysis of ROS and FAP expression. The percentage of cells in each quadrant is indicated. The numbers in brackets on the Y axis indicate CellROX signal intensity. (**f**) Volume of tumor xenografts with adoptively transferred ROS[high]/FAP[high]tFIBs and untransformed ROS[low]/FAP[low]FIBs. Mice, $n = 6$ per experimental condition. The data are presented as the mean $\pm$ S.D. *$P < 0.05$, **$P < 0.01$

PI3K/PKBα and ERK pathways when catalase was present (Figure 3c, Supplementary Figure S3A). The number of Ki67-positive proliferating epithelial cells was also reduced in the presence of catalase compared with the saline control (Figure 3d). Depletion of microenvironmental H_2O_2 by catalase partially restored basement membrane integrity between the epithelial layer and the adjacent stroma, as shown by a clear laminin 332 staining pattern, suggesting a reduced risk of malignancy (Figure 3d). To determine whether extratumoral H_2O_2 transforms normal FIBs into a CAF-like phenotype *in vivo*, we examined intracellular ROS levels and FAP expression in VybrantDiO-labeled FIBs isolated from tumor xenografts by FACS analysis (Supplementary Figure S3B). We observed that 10% of the cells were ROS^{high}/FAP^{high}FIBs, herein referred to as transformed FIBs (tFIBs), compared with only 3% tFIBs in the presence of catalase (Figure 3e). Next, we asked whether the tFIBs had tumor-promoting capabilities compared with untransformed FIBs (ROS^{low}/FAP^{low}). To this end, we performed an adoptive transfer of tFIBs and untransformed FIBs into new tumor xenografts (Figures 3f and g). We observed rapid xenograft growth when cancerous A-5RT3 cells were co-injected with tFIBs compared with FIBs. Non-tumorigenic HaCaT cells also grew at an accelerated rate when co-injected with tFIBs compared with FIBs (Figure 3f). Immunofluorescence staining further confirmed a more proliferative and aggressive epithelial cell phenotype in the presence of tFIBs (Figure 3g). Moreover, adoptively transferred tumors comprising A-5RT3 cells and tFIBs exhibited slower growth and less invasion in the presence of extracellular catalase compared with controls (Supplementary Figure S3C). Taken together, our *in vitro* and *in vivo* observations suggest that ROS, specifically H_2O_2, induce an oxidative CAF-like state in FIBs for stromal-mediated field cancerization.

Impaired TGFβ signaling reduces GPX1 expression in fibroblasts to cause a defect in ROS detoxification. Next, we investigated how extratumoral H_2O_2 activated FIBs to participate in field cancerization. TGFβ is a potent mediator of FIB activation, which signals through the canonical Smad and non-canonical TGFβ-activated kinase-1 (TAK1) pathways. We showed that exogenous H_2O_2 had similar activating effects on FIBs, such as elevated ROS levels, increased FAP and αSMA expression and reduced GSH:GSSG ratio (Figures 2j-l, Supplementary Figure S2F). Next, we probed the effect of H_2O_2 on fibroblast TGFβ signaling. A luciferase assay for TGFβ response revealed that CAFs have impaired TGFβ signaling, and FIBs became desensitized to TGFβ after 2 and 3 days of H_2O_2 treatment (Figure 4a). Correspondingly, Smad3 and TGFβRII mRNA expression in FIBs decreased after 2 and 3 days of H_2O_2 treatment, and TAK1 mRNA expression decreased after 3 days of H_2O_2 treatment (Figure 4b). FIBs treated with CCM showed similar impairment of TGFβ signaling, which was rescued by treatment with NAC (Figures 4a and b).

Oxidative stress also triggers NFκB activity in fibroblasts, leading to a CAF-like phenotype.[21,22] Indeed, FIBs treated with exogenous H_2O_2 displayed a significant increase in p65-NFκB phosphorylation after 2 and 3 days of $H_2O_2$ treatment (Supplementary Figure S3D). siRNA silencing of p65-NFκB expression in FIBs partially abrogated the H_2O_2-mediated suppression of Smad3, TAK1 and TGFβ mRNA and protein expression (Supplementary Figures S3E-G). These findings suggest that FIBs exposed to H_2O_2 initially remain responsive to TGFβ and this facilitates their activation and acquisition of FAP expression at an early time point, after just 1 day of H_2O_2 treatment. Simultaneously, H_2O_2 triggers NFκB activation that negatively regulates TGFβ signaling while potentiating FIB activation. NFκB activation is elevated after 2 days of H_2O_2 exposure, thus NFκB maintains FAP expression (and therefore, the CAF-like state) in H_2O_2-treated FIBs at later time points when TGFβ signaling becomes impaired.

To determine whether FIBs with impaired TGFβ signaling promote the growth of adjacent epithelia, we performed siRNA knockdown of Smad3 (F_{Smad3}), TAK1 (F_{TAK1}) and TGFβRII ($F_{TGF\beta RII}$) in FIBs and measured mitogenic factor secretion and ROS levels. The efficiency of siRNA knockdown was validated by qPCR and immunoblotting (Figures 4c and d). Compared with F_{ctrl}, no differences in proliferation or apoptosis of knockdown fibroblasts were observed by FACS analysis (Supplementary Figure S4A). We examined the secreted growth factor protein profile in CCM from these knockdown fibroblasts by ELISA. Out of a total of 76 distinct proteins screened, the expression levels of 7 secreted factors were elevated (Supplementary Figure S4B). A comparative analysis revealed that these factors were differentially modulated by Smad3 and TAK1 in FIBs (Supplementary Figure S4B). To further strengthen our observation, focused real-time PCR arrays comparing epithelia cocultured with CAFs and the various knockdown FIBs were performed. Notably, the expression profiles of many pro-oncogenic or tumor-associated genes in the epithelia cocultured with CAFs were also observed in the epithelia cocultured with F_{Smad3}, F_{TAK1}, $F_{TGF\beta RII}$ or treated with H_2O_2 (Supplementary Figure S1F). Importantly, immunoblot analysis of the epithelial layers of organotypic cocultures of keratinocytes with various knockdown fibroblasts showed the activation of the PI3K/PKB and ERK pathways associated with elevated epithelial proliferation, as indicated by PCNA (Supplementary Figure S4C). Next, we measured ROS levels in knockdown fibroblasts. Compared with F_{ctrl}, ROS levels were elevated in F_{Smad3} (8.9-fold), F_{TAK1} (8.4-fold) and $F_{TGF\beta RII}$ (8.2-fold) (Figures 4e and f). We also detected a significant increase in extracellular H_2O_2 from the knockdown fibroblasts compared with F_{ctrl}. The concentration of extracellular H_2O_2 was derived using a calibration curve created using known H_2O_2 concentrations (Figure 4g). $F_{TGF\beta RII}$ exhibited the highest amount of extracellular H_2O_2 (Figure 4g).

To investigate how impaired TGFβ signaling increases H_2O_2 levels in FIBs, we examined the expression of key enzymes affecting H_2O_2 detoxification in FIBs, namely, catalase, superoxide dismutase (SOD) and glutathione peroxidase (Gpx), using real-time PCR. No significant changes were observed in the mRNA levels of SOD1, SOD2 or catalase (Figure 4h). Interestingly, the mRNA and protein expression levels of Gpx1 were reduced in F_{Smad3}, F_{TAK1} and $F_{TGF\beta RII}$ compared with F_{ctrl}. H_2O_2 treatment of FIBs also resulted in an initial spike followed by a gradual loss of Gpx1 expression, corresponding to impaired TGFβ signaling (Figure 4b). Consistent with the qPCR data, Gpx protein expression and activity were reduced in CAFs

and fibroblasts with impaired TGFβ signaling, suggesting that the *GPx1* gene is regulated by Smad3- and TAK1-mediated pathways (Figures 4h and i). These observations indicate that epithelial cells are bathed in an oxidative microenvironment supplemented with mitogenic factors secreted by stromal fibroblasts with impaired TGFβ signaling.
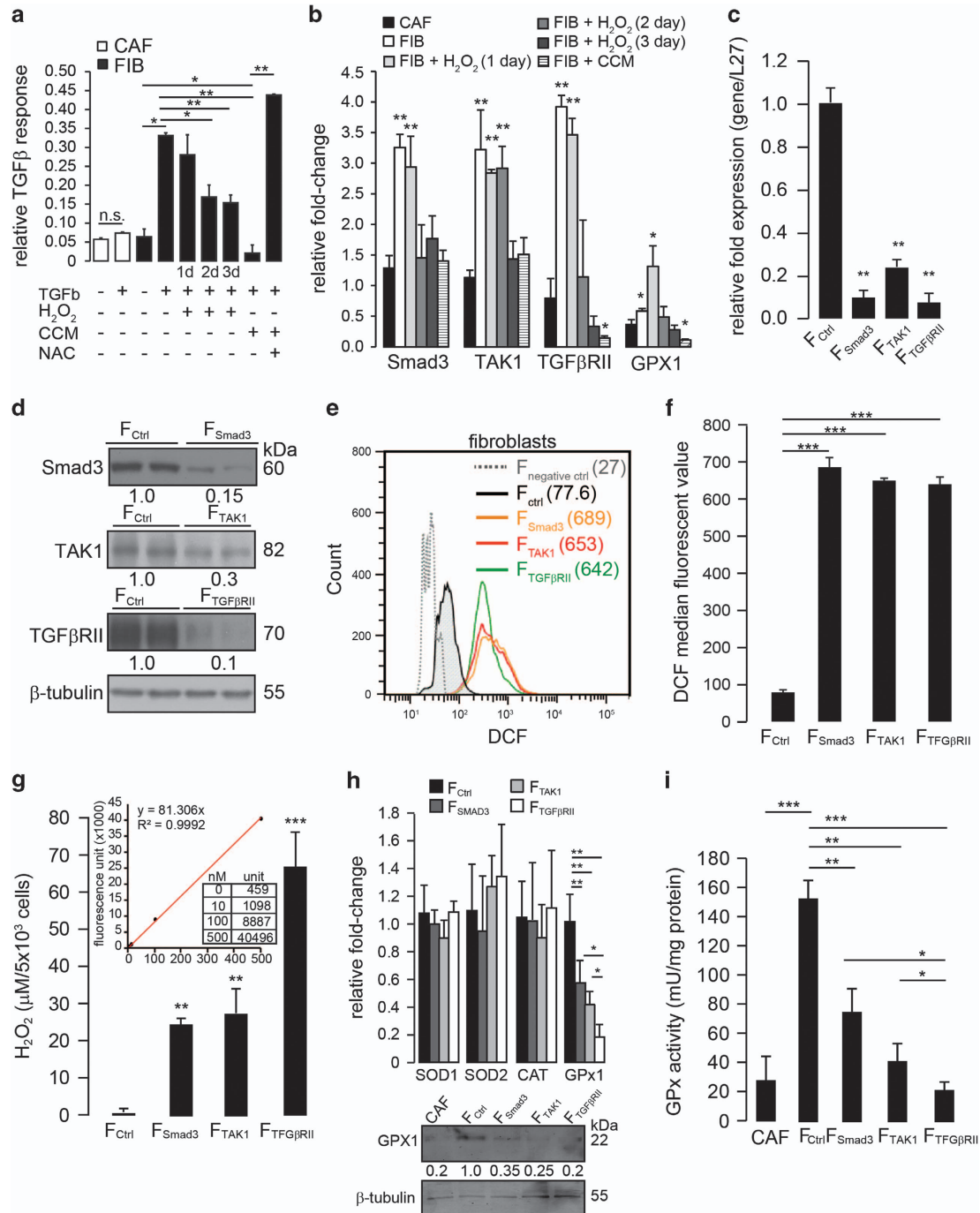
Figure 4 Impaired TGFβ signaling reduces GPX1 expression in FIBs to cause a defect in ROS detoxification. (**a**) Relative TGFβ-responsive reporter (luciferase) readings of FIBs and CAFs subjected to the indicated treatments followed by assay for TGFβ response. (**b** and **c**) Relative Smad3, TAK1, TGFβRII and GPX1 mRNA levels in FIBs and CAFs after the indicated treatments. The ribosomal RNA gene Rpl27 served as the housekeeping gene. (**d**) Immunoblot for Smad3, TAK1 and TGFβRII protein expression in control (scrambled) FIBs and siRNA knockdown FIBs. β-Tubulin from the same samples was used as a loading and transfer control. (**e** and **f**) Levels of ROS in FIBs with siRNA knockdown of Smad3, TAK1 and TGFβRII as determined by DCF staining and FACS. (**e**) The values in brackets indicate the mean fluorescence signal intensities. (**f**) Median DCF fluorescence intensity. (**g**) Extracellular H₂O₂ in conditioned medium from various knockdown FIBs as measured by Amplex Red assay. The figure insert shows the calibration curve for determining H₂O₂ concentration. (**h**) Relative SOD1, SOD2, CAT and GPx1 mRNA levels in knockdown FIBs. Rpl27 served as the housekeeping gene. Immunoblot of the GPx1 protein from the indicated cell lysates. β-Tubulin from the same samples was used as a loading and transfer control. (**i**) GPx1 activity measurements for the indicated cells normalized against total protein in the cell lysates. The data are presented as the mean ± S.D. of three independent experiments. *$P < 0.05$, **$P < 0.01$, ***$P < 0.001$

Regulation of Gpx1 by cJUN and Smad3 in CAFs from SCCs. *In silico* analysis of the human *GPx1* proximal promoter revealed two putative AP1-binding sites and one SMAD3-binding site (Figure 5a).[23,24] TAK1 is also a strong activator of cJun N-terminal kinase, which consequently activates cJUN. To determine whether *GPx1* is a target gene of cJUN and Smad3, chromatin immunoprecipitation (ChIP) experiments for cJUN and Smad3 followed by re-ChIP for p300, a cJUN and Smad3 coactivator, were performed. No binding of phospho-cJUN was detected at AP1(−12), indicating that this binding site is non-functional (Supplementary Figure S5A). There was amplification of the
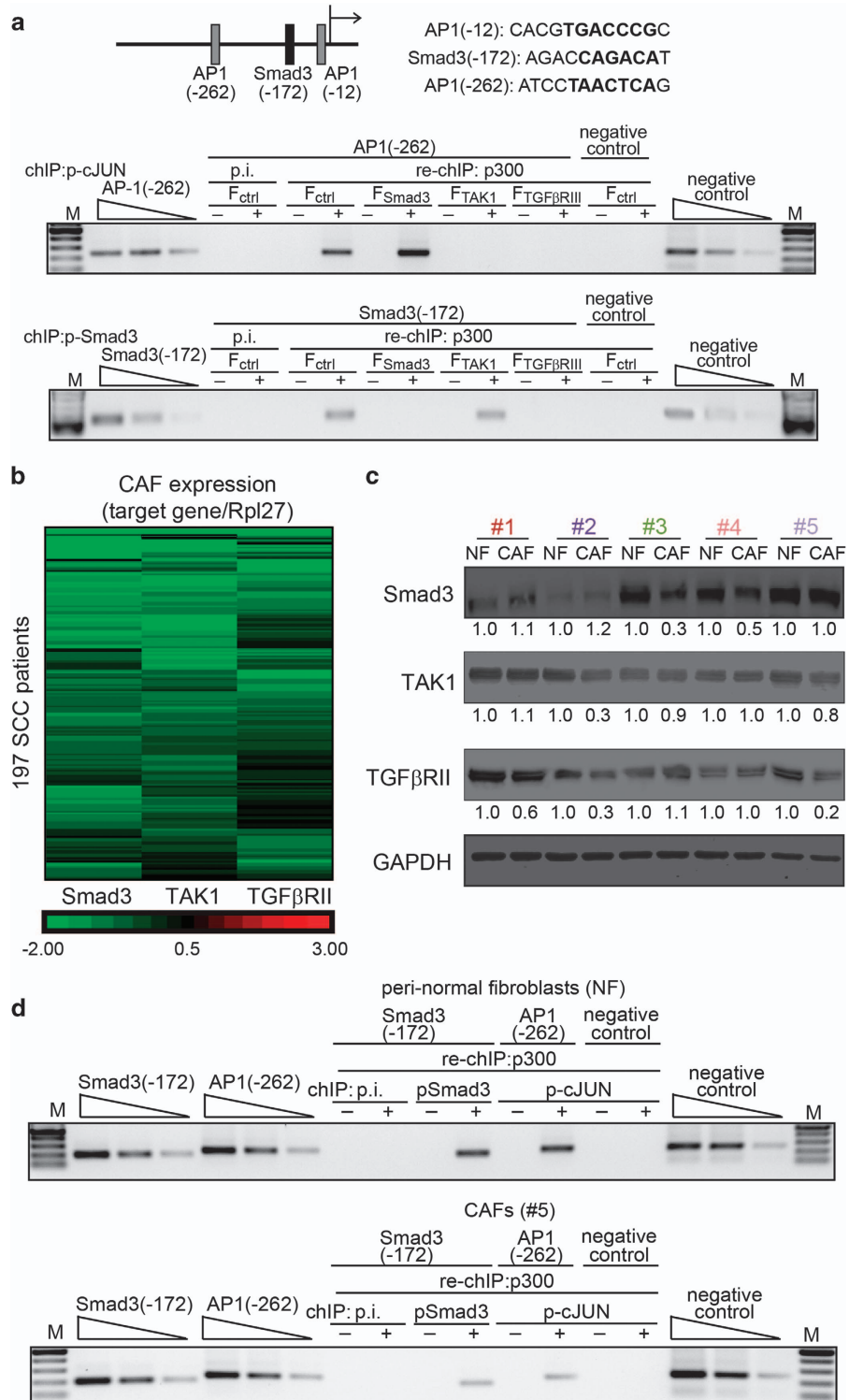
AP1(-262)-binding site in the human *GPx1* promoter after ChIP for phospho-cJUN (Supplementary Figure S5A) and re-ChIP for p300 in F_{ctrl} and F_{Smad3}, but not in F_{TAK1} and $F_{TGF\beta RII}$ (Figure 5a). There was also amplification of the Smad3 (-172)-binding site after ChIP for phospho-Smad3 (Supplementary Figure S5A) and re-ChIP for p300 in F_{ctrl} and F_{TAK1}, but not in F_{Smad3} and $F_{TGF\beta RII}$ (Figure 5a). No binding was detected with preimmune serum, and there was no binding to a control sequence ~ 2-kb upstream of the transcription start site. These observations indicate that the expression of the human *GPx1* gene in fibroblasts is regulated by canonical and non-canonical TGFβ-mediated signaling.

To underscore the clinical relevance of TGFβ signaling in stromal fibroblasts, we examined the mRNA expression of Smad3, TAK1 and TGFβRII in laser-microdissected CAFs from human SCC and adjacent peri-normal fibroblasts (NFs) from 197 patients. During microdissection, we collected the stroma (vimentin-positive) immediately associated with tumor epithelial cells rather than stromal tissue distal to the tumor, and excluded lymphocytes and obvious vascular structures. We observed reduced expression of Smad3, TAK1 and TGFβRII, alone or in combination, in CAFs compared with NFs (Figure 5b). Immunoblot analysis of these TGFβ signaling mediators in CAFs and cognate NFs isolated from five resected SCC samples selected at random from the available patient sample pool showed corresponding changes (Figure 5c). ChIP and re-ChIP experiments were also performed using NFs and CAFs (patient #5; reduced TGFβRII expression). Consistent with our earlier observations, the Smad3(-172) and AP1(-262)-binding sites of the human *GPx1* promoter were occupied by Smad3:p300 and cJUN:p300 in NFs, whereas their occupancies were significantly reduced in CAFs (Figure 5d, Supplementary Figure S4B). These results collectively indicate that impaired TGFβ signaling is a clinical feature of CAFs and is responsible for their loss of *GPx1* expression and activity, which consequently leads to micro-environmental oxidative stress and field cancerization.

Discussion

CAFs are one of the most abundant stromal cells in the tumor microenvironment, facilitating the development, propagation, and invasiveness of tumors.[25] Our study showed that CAF-derived ROS, specifically H_2O_2, induced oxidative stress in normal FIBs and trigger *de novo* CAF transformation *in vitro* and *in vivo*. Adoptive transfer of oxidatively tFIBs into malignant and non-tumorigenic epithelia xenografts resulted in faster-growing and more aggressive tumors, indicating exacerbated oncogenic transformation. This self-amplifying, field cancerization effect was due to impaired TGFβ signaling, leading to deficient *GPx1* expression and activity in CAFs. We showed that the human *GPx1* gene was regulated by TGFβ1-mediated Smad3 and TAK1/cJUN pathways in fibroblasts. Reduced expression of Smad3, TAK1 or TGFβRII was also detected in CAFs from a cohort of 197 SCC patients.

Fibroblast-specific deletion of TGFβRII in mice led to spontaneous tumors in the prostate and forestomach, which was partially attributed to the activation of paracrine HGF signaling.[26,27] However, TGFβ is required for fibroblast activation and transition to a CAF-like state. To reconcile these paradoxical observations, we noted that TGFβ signaling operates in a negative feedback loop mediated by the inhibitory Smad, Smad7,[28,29] which is upregulated by TGFβ via the pro-inflammatory transcription factor NFκB.[30,31] Oxidative stress is also strongly associated with NFκB activation.[32,33] Hence, FIBs exposed to H_2O_2 are initially responsive to TGFβ, which facilitates their activation by tumor epithelia- and CAF-derived TGFβ. Simultaneously, H_2O_2 triggers NFκB activation to suppress TGFβ signaling and GPx1 expression while potentiating FIB activation. In mature tumors, TGFβ is abundant and the tumor microenvironment is chronically subjected to low-grade inflammation and redox imbalance. These combined characteristics synergistically create an ecosystem that encourages the conversion of FIBs to CAFs, then renders CAFs refractory to TGFβ signaling and highly oxidative because of *Gpx1* deficiency. The expression of *Gpx1* is also regulated by p53,[34] and the ablation or mutation of p53 in stromal fibroblasts increased growth and metastatic spread of PC3 prostate cancer cells because of increased production of SDF-1.[35] Although the redox status of p53-deficient fibroblasts is unknown, it is conceivable that elevated H_2O_2 may contribute to their pro-tumorigenic effect. Together with our own observation that silencing NFκB expression could prevent the H_2O_2-mediated impairment of TGFβ signaling in fibroblasts, these findings suggest that transcriptional control has a critical role in modulating the pro-tumorigenic effects of CAFs.

Recent studies have revealed an important relationship between the extracellular redox state and cancer aggressiveness.[9] The activation of oncogenes in epithelial cells results in the loss of caveolin-1 and the elevated expression of lactate transporters in stromal fibroblasts. These CAF-like fibroblasts exhibited increased ROS levels and elevated glucose uptake, which complement cancer cell metabolism.[26,36] We showed that extratumoral H_2O_2, either

Figure 5 Regulation of Gpx1 by cJUN and Smad3 in CAFs from skin SCCs. (**a**) Schematic of the human *Gpx1* regulatory region showing the positions of the two putative AP1-binding sites and a Smad3-binding site relative to the transcription start site. The sequences of the sites are shown below. Representative ChIP results using anti-phospho-cJUN and anti-phospho-Smad3 antibodies followed by re-ChIP for anti-p300 in F_{Smad3}, F_{TAK1}, $F_{TGF\beta RII}$ and F_{ctrl}. Preimmune serum (p.i.) was used as the control for ChIP. $-/+$ Indicate vehicle and TGFβ treatment, respectively. The data are representative of $n = 3$ independent experiments. (**b**) Relative mRNA levels of TGFβ signaling mediators in a cohort of 197 patients. Fold changes are relative to the cognate NFs. Rpl27 served as the housekeeping gene. The qPCR data shown are from $n = 3$ experiments performed in triplicate. (**c**) The relative protein levels of TGFβ signaling mediators in paired CAFs and NFs from five human SCCs selected at random from the available sample pool for protein analysis. The immunoblot data are from three independent experiments performed in duplicate. GAPDH from the same samples served as a loading and transfer control. The values represent the mean fold differences compared with the cognate NFs. (**d**) Representative ChIP results using anti-phospho-cJUN and anti-phospho-Smad3 antibodies, followed by re-ChIP for anti-p300 using NFs and CAF#5. P.i. was used as the control for ChIP. The data are representative of $n = 3$ independent experiments. CAF#5 showed reduced TGFβRII expression

from epithelial tumor cells or CAFs, reinforced the already dysregulated epithelial–mesenchymal communication to promote field cancerization. Indeed, the prolonged exposure of primary human keratinocytes to low levels of H_2O_2 elevated the levels of oxidatively modified PTEN and Src, which triggered oncogenic signaling to promote epithelial transformation and growth; oxidization of the tumor suppressor PTEN and the oncogene Src results in protein inactivation and activation, respectively. H_2O_2 can also differentially influence the proliferation and invasiveness of cancer cells at various stages of progression. Lending support to a pro-mitogenic role of H_2O_2, H_2O_2 antagonized the cytostatic functions of TGFβ1 by the activation of Akt-ERK1/2-linked signaling.[37] Although the precise target of H_2O_2 was not identified, many studies have shown that Akt-ERK1/2 are downstream mediators of Src and PTEN.[34,38] Similarly, the migration of MCF-7 breast cancer cells was enhanced by elevated Nox4 expression in a human mammary fibroblast cell line.[36] Nox4 is known to predominantly produce H_2O_2 rather than O^{2-}.[39]

Finally, CAFs exert their proneoplastic activity by secreting mitogenic factors. Many of these factors are potential druggable targets, and it has been proposed that the inhibition of these ligand/receptor-activated signaling networks could limit neoplastic growth. We detected an increase in pro-mitogenic factors such as HGF and FGF7 in the conditioned media harvested from keratinocytes cocultured with fibroblasts with impaired TGFβ signaling. These elevated mitogenic factors, together with extracellular H_2O_2, promoted cancer cell proliferation, as supported by the activation of pro-oncogenic PKBα, ERK and JNK pathways in the epithelia. Our findings that the oxidative action of H_2O_2 also enables CAF-mediated field cancerization suggest that anticancer strategies that singularly target the ligand-receptor pathways may not be effective. For example, a neutralizing antibody to HGF exhibited potent antitumor effect in the treatment of glioblastoma multiforme.[40] However, tumor growth became HGF-independent after repeated treatments.[41] Conceivably, the promiscuous nature of H_2O_2 interactions with cellular signaling components, especially membrane-associated molecules such as EGFR and Met, renders the cells less dependent on ligand-activated pathways to promote transformation and growth. Indeed, initial efforts focused on the inhibition of PDGF with a single agent, imatinib, generated poor outcomes.[42,43] In contrast, combination treatment with hydroxyurea and imatinib has provided very encouraging findings.[44,45] Interestingly, hydroxyurea is a potent antioxidant that has been shown to increase the expression of *Gpx1* in a p53-dependent manner, among other effects.[46] Future exploration of new multi-modal approaches that simultaneously target ligand-receptor signaling and redox-mediated pathways will offer new promising anticancer strategies.

Materials and Methods

Human tumor samples. Human SCC biopsies along with their paired peri-normal tissues were provided by the National Skin Centre, Singapore. CAFs and FIBs were isolated by laser capture microdissection and subjected to protein and RNA extraction for immunoblotting and real-time PCR analyses, respectively.[47,48] The study was approved by the National Healthcare Group Domain-Specific Review Boards (NHG-DSRB). All tumor samples were de-identified before the analyses.

***In vitro* tumor colony promotion protocol.** Keratinocytes were seeded at a density of 1×10^5 per 35-mm dish containing complete OTC medium (Denova Sciences, Singapore) at day 0. On day 1, cultures were treated for 1 h with the initiating agent, MNNG, or solvent control (DMSO). The cells were washed, and the medium was replaced with complete medium for 24 h before exposure to different concentrations of H_2O_2. After 1 week, cells were harvested from individual dishes and passaged at a density of 1×10^5 per 35-mm dish in H_2O_2-containing medium. Concurrently, 2×10^4 harvested cells were embedded in 0.35% noble agar (Sigma Aldrich, St. Louis, MO, USA) and layered onto 0.7% noble agar-coated 35-mm dishes during each passage of the cells. These soft agar cultures were consistently replenished with fresh H_2O_2-containing medium every other day. After 1 month, viable transformed colonies were stained with 1 mg/ml thiazolyl blue tetrazolium in PBS and counted.

Cell proliferation, apoptosis assays and FACS analysis. Bromo-deoxyuridine (BrdU) incorporation and total DNA content in proliferating cells were analyzed by BrdU and PI staining using the BrdU Flow kit (BD Biosciences, San Jose, CA, USA). Epithelial cells were treated for 24 h with the indicated concentrations of H_2O_2 in serum-free medium. The cells were incubated with BrdU (40 μM) for 30 min. Apoptotic and necrotic cells were quantified using an Annexin V/PI staining kit (BioLegend, San Diego, CA, USA) and subsequent FACS analysis.

PEG-switch assay and OxyBlot protein oxidation detection. PEG-switch assay was performed as previously described.[49] Cells treated with 100 nM H_2O_2 or 10 ng/ml MNNG for 24 h were lysed using M-PER mammalian protein extraction reagent (Thermo Fisher Scientific, Waltham, MA, USA). Oxidized thiols were reduced using DTT and alkylated using 2 mM PEG-maleimide with 0.5% SDS for 2 h at room temperature. The alkylation reaction was quenched using 100 mM Tris–HCl buffer pH 6.8, 4% SDS, 20% glycerol, and 0.01% bromophenol blue and 100 mM maleimide and the samples were resolved by SDS-PAGE and subjected to immunoblot. Oxidatively modified PTEN was analyzed as previously described with some modifications.[17] Cells treated with 100 nM H_2O_2 for 30 min were washed with oxygen-free ice-cold PBS containing 1 mM *N*-ethylmaleimide (NEM). Cells were lysed in lysis buffer (50 mM Tris, pH 6.8, 150 mM NaCl, 1 mM EDTA, 0.5% Triton X-100 and 30 mM NEM). Lysates were further clarified using aQIAshredder (Qiagen, Valencia, CA, USA). Equal amounts of proteins were mixed with NEM loading dye (50 mM Tris, pH 6.8, 10% glycerol, 2% SDS, 20 mM NEM and 0.02% bromophenol blue) and resolved by non-reducing SDS-PAGE. As a control, proteins were completely reduced by heating in SDS-loading dye containing DTT. Oxidized Src was detected as previously described.[19] The separated proteins were subjected to immunoblot analysis using antibodies against PTEN and Src.

H_2O_2 and CCM treatment of FIBs *in vitro*. FIBs and CAFs were seeded at a density of 1×10^4 per 35-mm dish in FibroGRO-LS (Millipore, Billerica, MA, USA). The 48-h CCM was collected from CAFs, sterile filtered and used immediately. CCM, with or without 100 μM *N*-acetylcysteine (Sigma Aldrich) pretreatment, was added to wells containing FIBs and refreshed daily over 3 days, after which FIBs were harvested for FACS analysis. Separately, FIBs were treated with 100 nM H_2O_2 in serum-free FibroGRO-LS for 30 min twice daily with an 8-h interval between treatments for a maximum of 3 days. FIBs were harvested for FACS analysis 24 h after 1 day, 2 days and 3 days of H_2O_2 treatment.

***In vivo* tumor growth and adoptive transfer of tFIBs.** A total of 1×10^5 HaCaT or A-5RT3 cells were admixed with 2×10^5 CAFs and 1×10^5 VybrantDiO (Life Technologies, Waltham, MA, USA)-labeled FIBs in growth factor-reduced Matrigel (Corning, Tewksbury, MA, USA), with or without 500 U/ml catalase (Sigma), and implanted subcutaneously into NSG mice (Jackson Laboratory, Bar Harbor, ME, USA) (Figure 3a). Three weeks post-implantation, tumors were excised and dissociated using the MACS tumor dissociation kit and a gentleMACS Octo Dissociator (Miltenyi Biotec, Germany). Then, the tumors were doubly stained with CellROX Deep Red (Thermo, Waltham, MA, USA) and PE-conjugated anti-FAP antibody (Novus Biologicals, Littleton, CO, USA) for FACS. A total of 3×10^5 ROS^{high}/FAP^{high}tFIBs were isolated and adoptively transferred into new tumor xenografts containing either HaCaT or A-5RT3 cells. Tumor growth was monitored for 3 weeks. All animal studies were approved by the Institutional Animal Care and Use Committee of Nanyang Technological University (ARF-SBS/NIE-A0216AZ).

ChIP and re-ChIP. ChIP was performed using phospho-cJUN and phospho-Smad3 antibodies (Cell Signaling, Danvers, MA, USA), and re-ChIP was performed using a p300 antibody (Upstate Biotechnology, Lake Placid, NY, USA) as previously described.[50] The primer sequences are listed in Supplementary Table S1.

Immunoblot assay. Far-infrared immunoblotting was performed as previously described.[51]

Measurement of extracellular H_2O_2, intracellular ROS and GSH/GSSG ratio. Extracellular H_2O_2 and intracellular ROS were measured as previously described.[47,52] The specificity of the assay for H_2O_2 was verified with catalase, and the degradation of H_2O_2 or inhibition of the assay system by the sample was analyzed by determining the recovery of exogenously added H_2O_2. GSH/GSSG ratio was measured using the GSH/GSSG ratio detection assay kit green (Abcam, Cambridge, UK) according to the manufacturer's recommendations.

Mitogenic factor array. The expression profiles of the secreted factors present in the conditioned medium (48 h) were identified using the RayBio Human Growth Factor Array 1 and Human Inflammation Antibody Array 3 (RayBiotech, Inc., Norcross, GA, USA). These membranes were incubated with conditioned media from the different cocultures and then processed.

Statistical analysis. Statistical differences were determined using a two-tailed Mann–Whitney *U*-test. A *P*-value of < 0.05 was considered statistically significant.

Conflict of Interest

The authors declare no conflict of interest.

1. Tlsty TD, Hein PW. Know thy neighbor: stromal cells can contribute oncogenic signals. *Curr Opin Genet Dev* 2001; **11**: 54–59.
2. Udagawa T, Wood M. Tumor-stromal cell interactions and opportunities for therapeutic intervention. *Curr Opin Pharmacol* 2010; **10**: 369–374.
3. Franco OE, Shaw AK, Strand DW, Hayward SW. Cancer associated fibroblasts in cancer pathogenesis. *Semin Cell Dev Biol* 2010; **21**: 33–39.
4. Olumi AF, Grossfeld GD, Hayward SW, Carroll PR, Tlsty TD, Cunha GR. Carcinoma-associated fibroblasts direct tumor progression of initiated human prostatic epithelium. *Cancer Res* 1999; **59**: 5002–5011.
5. Shimoda M, Mellody KT, Orimo A. Carcinoma-associated fibroblasts are a rate-limiting determinant for tumour progression. *Semin Cell Dev Biol* 2010; **21**: 19–25.
6. Braakhuis BJ, Tabor MP, Kummer JA, Leemans CR, Brakenhoff RH. A genetic explanation of Slaughter's concept of field cancerization: evidence and clinical implications. *Cancer Res* 2003; **63**: 1727–1730.
7. Rivenbark AG, Coleman WB. Field cancerization in mammary carcinogenesis - implications for prevention and treatment of breast cancer. *Exp Mol Pathol* 2012; **93**: 391–398.
8. Dotto GP. Multifocal epithelial tumors and field cancerization: stroma as a primary determinant. *J Clin Invest* 2014; **124**: 1446–1453.
9. Chaiswing L, Oberley TD. Extracellular/microenvironmental redox state. *Antioxid Redox Signal* 2010; **13**: 449–465.
10. Lisanti MP, Martinez-Outschoorn UE, Chiavarina B, Pavlides S, Whitaker-Menezes D, Tsirigos A *et al*. Understanding the "lethal" drivers of tumor-stroma co-evolution: emerging role(s) for hypoxia, oxidative stress and autophagy/mitophagy in the tumor micro-environment. *Cancer Biol Ther* 2010; **10**: 537–542.
11. Liou GY, Storz P. Reactive oxygen species in cancer. *Free Radic Res* 2010; **44**: 479–496.
12. Ray PD, Huang BW, Tsuji Y. Reactive oxygen species (ROS) homeostasis and redox regulation in cellular signaling. *Cell Signal* 2012; **24**: 981–990.
13. Zhang Y, Du Y, Le W, Wang K, Kieffer N, Zhang J. Redox control of the survival of healthy and diseased cells. *Antioxid Redox Signal* 2011; **15**: 2867–2908.
14. Baker MS, Gebicki JM. The effect of pH on the conversion of superoxide to hydroxyl free radicals. *Arch Biochem Biophys* 1984; **234**: 258–264.
15. Takahashi MA, Asada K. Superoxide anion permeability of phospholipid membranes and chloroplast thylakoids. *Arch Biochem Biophys* 1983; **226**: 558–566.
16. Boukamp P, Popp S, Bleuel K, Tomakidi E, Bürkle A, Fusenig NE. Tumorigenic conversion of immortal human skin keratinocytes (HaCaT) by elevated temperature. *Oncogene* 1999; **18**: 5638–5645.

17. Lee SR, Yang KS, Kwon J, Lee C, Jeong W, Rhee SG. Reversible inactivation of the tumor suppressor PTEN by H2O2. *J Biol Chem* 2002; **277**: 20336–20342.
18. Kwon J, Lee SR, Yang KS, Ahn Y, Kim YJ, Stadtman ER *et al*. Reversible oxidation and inactivation of the tumor suppressor PTEN in cells stimulated with peptide growth factors. *Proc Natl Acad Sci USA* 2004; **101**: 16419–16424.
19. Giannoni E, Buricchi F, Raugei G, Ramponi G, Chiarugi P. Intracellular reactive oxygen species activate Src tyrosine kinase during cell adhesion and anchorage-dependent cell growth. *Mol Cell Biol* 2005; **25**: 6391–6403.
20. Giannoni E, Chiarugi P. Redox circuitries driving Src regulation. *Antioxid Redox Signal* 2014; **20**: 2011–2025.
21. Erez N, Truitt M, Olson P, Arron ST, Hanahan D. Cancer-associated fibroblasts are activated in incipient neoplasia to orchestrate tumor-promoting inflammation in an NF-kappaB-dependent manner. *Cancer Cell* 2010; **17**: 135–147.
22. Martinez-Outschoorn U, Sotgia F, Lisanti MP. Tumor microenvironment and metabolic synergy in breast cancers: critical importance of mitochondrial fuels and function. *Semin Oncol* 2014; **41**: 195–216.
23. Seldeen KL, McDonald CB, Deegan BJ, Farooq A. Single nucleotide variants of the TGACTCA motif modulate energetics and orientation of binding of the Jun-Fos heterodimeric transcription factor. *Biochemistry* 2009; **48**: 1975–1983.
24. Jonk LJ, Itoh S, Heldin CH, ten Dijke P, Kruijer W. Identification and functional characterization of a Smad binding element (SBE) in the JunB promoter that acts as a transforming growth factor-beta, activin, and bone morphogenetic protein-inducible enhancer. *J Biol Chem* 1998; **273**: 21145–21152.
25. Mueller MM, Fusenig NE. Tumor-stroma interactions directing phenotype and progression of epithelial skin tumor cells. *Differentiation* 2002; **70**: 486–497.
26. Lisanti MP, Martinez-Outschoorn UE, Sotgia F. Oncogenes induce the cancer-associated fibroblast phenotype: metabolic symbiosis and "fibroblast addiction" are new therapeutic targets for drug discovery. *Cell Cycle* 2013; **12**: 2723–2732.
27. Larue L, Bellacosa A. Epithelial-mesenchymal transition in development and cancer: role of phosphatidylinositol 3' kinase/AKT pathways. *Oncogene* 2005; **24**: 7443–7454.
28. Stroschein SL, Wang W, Zhou S, Zhou Q, Luo K. Negative feedback regulation of TGF-beta signaling by the SnoN oncoprotein. *Science* 1999; **286**: 771–774.
29. Papageorgis P, Stylianopoulos T. Role of TGFbeta in regulation of the tumor microenvironment and drug delivery (review). *Int J Oncol* 2015; **46**: 933–943.
30. Bitzer M, von Gersdorff G, Liang D, Dominguez-Rosales A, Beg AA, Rojkind M *et al*. A mechanism of suppression of TGF-beta/SMAD signaling by NF-kappa B/RelA. *Genes Dev* 2000; **14**: 187–197.
31. Freudlsperger C, Bian Y, Contag Wise S, Burnett J, Coupar J, Yang X *et al*. TGF-beta and NF-kappaB signal pathway cross-talk is mediated through TAK1 and SMAD7 in a subset of head and neck cancers. *Oncogene* 2013; **32**: 1549–1559.
32. Kratsovnik E, Bromberg Y, Sperling O, Zoref-Shani E. Oxidative stress activates transcription factor NF-kB-mediated protective signaling in primary rat neuronal cultures. *J Mol Neurosci* 2005; **26**: 27–32.
33. Gloire G, Legrand-Poels S, Piette J. NF-kappaB activation by reactive oxygen species: fifteen years later. *Biochem Pharmacol* 2006; **72**: 1493–1505.
34. Logue JS, Morrison DK. Complexity in the signaling network: insights from the use of targeted inhibitors in cancer therapy. *Genes Dev* 2012; **26**: 641–650.
35. Addadi Y, Moskovits N, Granot D, Lozano G, Carmi Y, Apte RN *et al*. p53 status in stromal fibroblasts modulates tumor growth in an SDF1-dependent manner. *Cancer Res* 2010; **70**: 9650–9658.
36. Tobar N, Guerrero J, Smith PC, Martinez J. NOX4-dependent ROS production by stromal mammary cells modulates epithelial MCF-7 cell migration. *Br J Cancer* 2010; **103**: 1040–1047.
37. Choi J, Park SJ, Jo EJ, Lee HY, Hong S, Kim SJ *et al*. Hydrogen peroxide inhibits transforming growth factor-beta1-induced cell cycle arrest by promoting Smad3 linker phosphorylation through activation of Akt-ERK1/2-linked signaling pathway. *Biochem Biophys Res Commun* 2013; **435**: 634–639.
38. Steelman LS, Chappell WH, Abrams SL, Kempf RC, Long J, Laidler P *et al*. Roles of the Raf/MEK/ERK and PI3K/PTEN/Akt/mTOR pathways in controlling growth and sensitivity to therapy-implications for cancer and aging. *Aging (Albany NY)* 2011; **3**: 192–222.
39. Bedard K, Krause KH. The NOX family of ROS-generating NADPH oxidases: physiology and pathophysiology. *Physiol Rev* 2007; **87**: 245–313.
40. Cao B, Su Y, Oskarsson M, Zhao P, Kort EJ, Fisher RJ *et al*. Neutralizing monoclonal antibodies to hepatocyte growth factor/scatter factor (HGF/SF) display antitumor activity in animal models. *Proc Natl Acad Sci USA* 2001; **98**: 7443–7448.
41. Zhao P, Gao C, Dykema K, Furge K, Feng Z, Cao B *et al*. Repeated hepatocyte growth factor neutralizing antibody treatment leads to HGF/SF unresponsiveness in human glioblastoma multiforme cells. *Cancer Lett* 2010; **291**: 209–216.
42. Ostman A, Heldin CH. PDGF receptors as targets in tumor treatment. *Adv Cancer Res* 2007; **97**: 247–274.
43. Wen PY, Yung WK, Lamborn KR, Dahia PL, Wang Y, Peng B *et al*. Phase I/II study of imatinib mesylate for recurrent malignant gliomas: North American Brain Tumor Consortium Study 99-08. *Clin Cancer Res* 2006; **12**: 4899–4907.
44. Reardon DA, Egorin MJ, Quinn JA, Rich JN, Gururangan S, Vredenburgh JJ *et al*. Phase II study of imatinib mesylate plus hydroxyurea in adults with recurrent glioblastoma multiforme. *J Clin Oncol* 2005; **23**: 9359–9368.
45. Dresemann G. Imatinib and hydroxyurea in pretreated progressive glioblastoma multiforme: a patient series. *Ann Oncol* 2005; **16**: 1702–1708.

46. Koncic MZ, Barbaric M, Perkovic I, Zorc B. Antiradical, chelating and antioxidant activities of hydroxamic acids and hydroxyureas. *Molecules* **16**: 6232–62422011.

47. Zhu P, Tan MJ, Huang RL, Tan CK, Chong HC, Pal M *et al.* Angiopoietin-like 4 protein elevates the prosurvival intracellular O2(-):H2O2 ratio and confers anoikis resistance to tumors. *Cancer Cell* 2011; **19**: 401–415.

48. Chong HC, Tan MJ, Philippe V, Tan SH, Tan CK, Ku CW *et al.* Regulation of epithelial-mesenchymal IL-1 signaling by PPARbeta/delta is essential for skin homeostasis and wound healing. *J Cell Biol* 2009; **184**: 817–831.

49. Burgoyne JR, Oviosu O, Eaton P. The PEG-switch assay: a fast semi-quantitative method to determine protein reversible cysteine oxidation. *J Pharmacol Toxicol Methods* 2013; **68**: 297–301.

50. Lam CR, Tan MJ, Tan SH, Tang MB, Cheung PC, Tan NS. TAK1 regulates SCF expression to modulate PKBalpha activity that protects keratinocytes from ROS-induced apoptosis. *Cell Death Differ* 2011; **18**: 1120–1129.

51. Chong HC, Chan JS, Goh CQ, Gounko NV, Luo B, Wang X *et al.* Angiopoietin-like 4 stimulates STAT3-mediated iNOS expression and enhances angiogenesis to accelerate wound healing in diabetic mice. *Mol Ther* 2014; **22**: 1593–1604.

52. Wang X, Sng MK, Foo S, Chong HC, Lee WL, Tang MB *et al.* Early controlled release of peroxisome proliferator-activated receptor beta/delta agonist GW501516 improves diabetic wound healing through redox modulation of wound microenvironment. *J Control Release* 2015; **197**: 138–147.

Supplementary Information accompanies this paper on Cell Death and Disease website (http://www.nature.com/cddis)